PRELIMINARY RESULTS FROM REFLECTANCE SPECTROSCOPY OBSERVATIONS OF SPACE DEBRIS IN GEO

Alessandro Vananti[(1)], Thomas Schildknecht[(1)], Holger Krag[(2)], Christian Erd[(3)]

[(1)]Astronomical Institute, University of Bern, Sidlerstrasse 5, CH-3012 Bern, Switzerland,
alessandro.vananti@aiub.unibe.ch, thomas.schildknecht@aiub.unibe.ch
[(2)]ESA/ESOC, Robert-Bosch-Strasse 5, D-64293 Darmstadt, Germany, holger.krag@esa.int
[(3)]ESA/ESTEC, Keplerlaan 1, NL-2200 Noordwijk, Netherlands, cerd@rssd.esa.int

ABSTRACT

The space debris environment in the Geostationary Earth Orbit (GEO) region is mostly investigated using optical telescopes. The detection of the objects and the determination of their orbits are based on optical observations. However, for a better characterization of the environment it would be necessary to know the shape and the material of the objects. The area-to-mass ratio can be estimated from orbit determinations. In some rare case additional information can be derived from photometric measurements. A possible technique to investigate the material type of the debris is the reflectance spectroscopy. This paper discusses preliminary results obtained from spectrometric observations of orbital space debris. The observations were acquired at the 1-meter ESA Space Debris Telescope (ESASDT) on Tenerife with a low-resolution spectrograph in the wavelength range of 450-960 nm. The observed objects are space debris in GEO orbits with brightness as small as magnitude 16. The spectra show shape variations expected to be caused by the different physical properties of the objects. The determination of the material and of the type of object is still in a preliminary phase. Limitations of the acquisition process of the spectra and the subsequent analysis are discussed. Future steps planned for a better characterization of the debris from the observed data are briefly outlined.

1. INTRODUCTION

The characterization of the space debris environment at high altitudes mostly involves optical observations. The debris surveys include the discovery of new objects, the determination and maintenance of their orbits, and possibly the investigation of the physical properties of these objects. Optical observations give little information on the size, shape and material of the debris. Different techniques permit to determine some aspects of the observed fragments, but each technique has its own limitation. Colour Photometry may be used to obtain an indication about the composition of fragmentation debris of one material type only. Photometric measurements and light curves might help to identify the rotation of an object and its rotation rate [1]. Sometimes the analysis of the orbits over long observation arcs allows estimating characteristics like the area-to-mass ratio of the observed objects [2]. Since these techniques have certain limitations, it is necessary to explore other methods to characterize the space debris. One promising approach is to collect debris data that are resolved in the spectral dimension. Reflectance spectrometry is the quantitative measurement of the reflection properties of a material as a function of the wavelength. The flux from an object is measured in different wavelengths and compared quantitatively with the solar spectral energy distribution. Different studies have already been conducted on reflectance spectroscopy of orbiting objects [3, 4]. In some studies the measured spectra are compared with laboratory measurements of the same object or satellite component. For some specific materials it is possible to identify characteristic spectral features, a sort of fingerprint. Furthermore it has been observed that the objects exposed to the space environment for long time exhibit space weathering effects. Their spectra show a so-called "reddening", that is an increase in slope of the reflectance with increasing wavelength [5]. In this work, reflectance spectroscopy measurements of objects in the geostationary region are shown. The selected objects consist, on one hand, of satellites whose shape and size are known and on the other hand of small faint debris with brightness up to magnitude 16. Among the latter category there are some objects with high area-to-mass ratio.

2. EQUIPMENT

The observations were performed at the 1-meter ESA Space Debris Telescope (ESASDT) on Tenerife with the ESA OGS Spectrograph. The low-resolution "GrismBB" was selected among the available dispersion components of the OGS spectrograph. The GrismBB has a wavelength range between 450 nm and 960 nm with a center wavelength of 510 nm and a dispersion of 0.4 nm/pixel at the center of the CCD. Due to the broad band width of the dispersion, the second order gets dispersed into the same spatial area. Therefore an additional order separation filter must be used for wavelengths larger than 550 nm. For this purpose a glass filter OG515 with a cut-off position of 515 nm was used. In the spectrograph optics a 5 arcsec slit was

employed. For the calibration the spectrograph system is equipped with an Osram He/10 spectral lamp. The measurements were acquired with a camera equipped with a backside illuminated CCD of 2048 x 2048 pixels and a pixel size of 13.5 x 13.5 μm^2.

3. OBSERVATIONS

The measurements were acquired on 11 nights during campaigns in November 2008 and January 2009. The program objects include the Meteosat satellites MSG1 and MSG2, the communication satellites Astra-1D and Artemis, as well as the minor planets Pomona and Nausikaa. In addition, a selection of debris objects from the catalogue at the Astronomical Institute of the University of Bern (AIUB) was chosen. The catalogue contains objects discovered during ESA debris surveys and their orbits are updated with follow-up observations at the ESASDT telescope and at AIUB's 1-meter telescope ZIMLAT in Zimmerwald (Switzerland). Additional observations are also provided by the International Scientific Optical Network (ISON) in the framework of a collaboration with the Keldysh Institute of Applied Mathematics (KIAM). The debris selected for the spectroscopy observations consists of objects in GEO and GTO orbits, and objects with high area-to-mass ratio. Their magnitudes vary from 13 to 16. The area-to-mass ratios range from small values around 0.01 m^2/kg up to very large values of more than 10 m^2/kg. All program and calibration objects were observed with and without the above-mentioned OG515 filter, to obtain spectra for wavelengths longer and shorter than 550 nm. After every object observation a calibration measurement with the He lamp was executed. Some objects were measured on several nights to acquire spectra for different phase angles. As reference stars for the spectrometric reductions the following solar analogs were observed: SA 93-101, SA 112-1333, SA 102-1081, SA 107-684, SA 98-978, and SAO 93936. The solar analog measurements were performed at regular intervals during the observation nights to collect calibration data at different air masses, which is important for atmospheric extinction determinations.

4. REDUCTION

The reduction of the data was performed with the standard ESO-MIDAS software package [6] developed by the ESO (European Southern Observatory). The long slit spectroscopy context "LONG" was selected from the available libraries. The one-dimensional spectra were extracted from the acquired frames using the "EXTRAC/AVER" command. In this procedure the pixel values are binned perpendicularly to the dispersion direction on the frame and averaged. Two different binning regions are selected on the frame, one for the background (sky spectrum) and one for the measured object. The background is then subtracted from the object spectrum. From the He-lamp calibration spectra the prominent peaks were searched and identified by means of the functions "SEARCH/LONG" and "IDENTI/LONG". The objects spectra were calibrated using "CALIBR/LONG" and "REBIN/LONG". The resulting spectra were normalized to 1 at 550 nm. After this step the spectra were corrected for atmospheric extinction. For this purpose solar analog spectra measured at different air mass values were used. To reduce the number of observations the solar analog were employed as spectral reference and also as extinction reference. Fig. 1 shows four different curves of solar analogs corresponding to increasing air masses. The extinction strongly influences the shape of the spectrum, the intensity at small wavelengths is highly reduced. For this reason the extinction must be accurately determined for every night. To calculate it, the intensities of the solar analog spectra are expressed as a function of the related air mass for different wavelengths. Eq. 1 represents the extinction law, where A is the air mass, I_0 and I are the intensities before and after the extinguishing medium, and $K(\lambda)$ is the extinction function. A linear fit of the air mass dependency expressed on a logarithmic scale yields the extinction for the corresponding wavelength. The fits were calculated with the "REGRE/LINE" function.

$$K(\lambda)\cdot A = -2.5\cdot \log\frac{I}{I_0} \qquad (1)$$

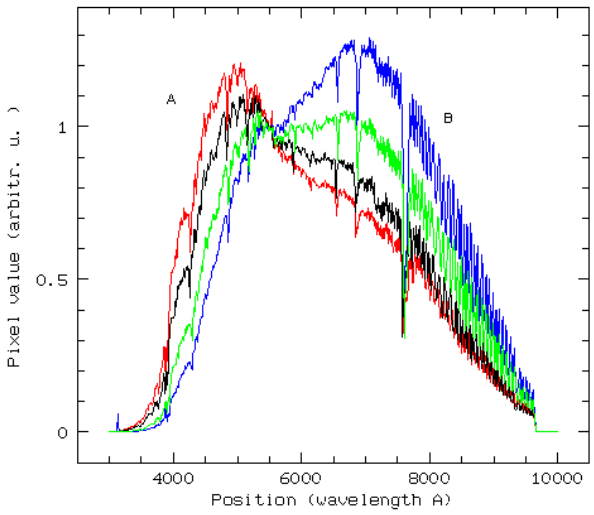

Figure 1. Normalized spectra of a solar analog measured at different air mass values (from A to B): 1.02, 1.13, 1.4, 1.94

Extinction curves of three different nights are showed in Fig. 2. The values can considerably vary from night to night.

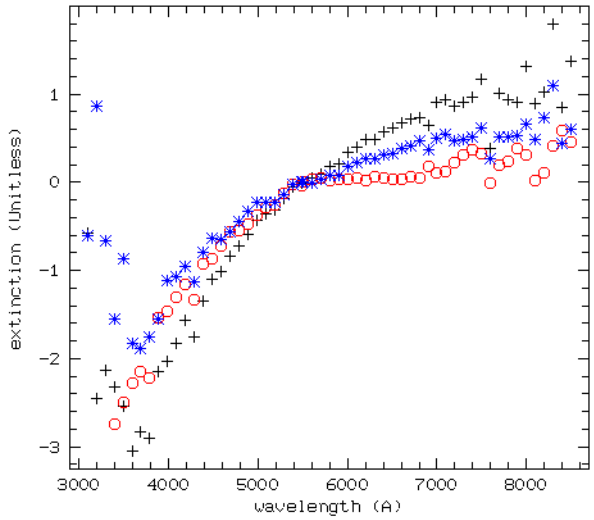

Figure 2. Extinction curves extracted from normalized solar analog spectra for three different nights

After the extinction correction of the spectra with "EXTINC/LONG", the object spectra were divided by the solar analog spectra to obtain intensity-calibrated reflectance spectra. This procedure also takes into account the spectrograph response function, since the latter is present in both measurements. Fig. 3 illustrates the observed spectra of an object, of a solar analog, and the resulting intensity-calibrated reflectance spectrum of the object.

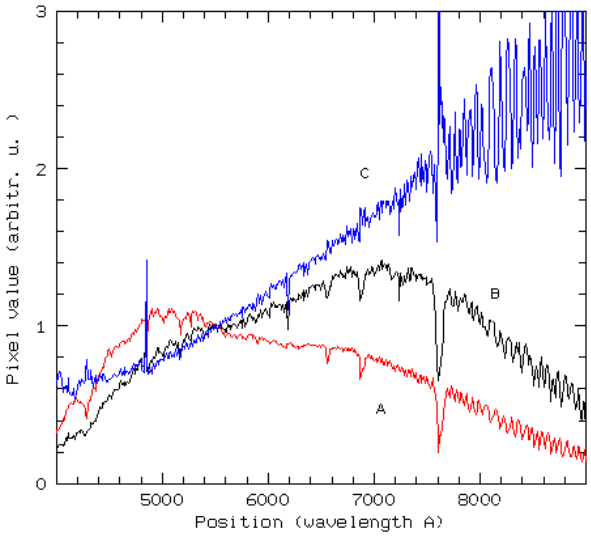

Figure 3. The observed spectrum of the object (A) is divided by the spectrum of the solar analog (B) to obtain the reflectance spectrum (C)

After the intensity calibration, the processed spectra measured without and with second-order filter were merged together. The data for wavelengths shorter than 550 nm was taken from the unfiltered spectra, while for longer wavelengths it was taken from the filtered ones. In the final step a low-pass filter was applied to the spectra with the function "FILTER/SMOO", to remove background noise and the effect of fringes. The latter arise from the interference of light, which is reflected multiple times between the upper and lower surface of the CCD.

5. RESULTS

The spectra of the selected objects show several characteristics, like peaks, slope variations, modulations, and different shapes. These "features" may possibly be used to distinguish the observed satellites or debris fragments. Fig. 4 shows the spectra of object S92005 taken on two different nights. This object is included in the AIUB catalogue, has magnitude 14 and resides on a Geostationary Transfer Orbit (GTO). The two spectra exhibit big similarities: an almost identical slope between 500 nm and 900 nm, a strong increase of the intensity below 400 nm, and several more or less smoothed peaks from 800 nm upwards. Obviously the reproducibility can be guaranteed only under the condition that the phase angle remains approximately constant and the object did not rotate or change its orientation between the two measurements.

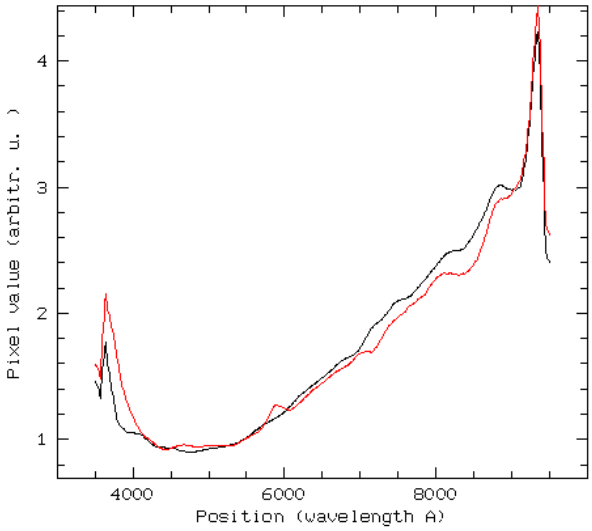

Figure 4. Spectrum of object S92005 taken on two different nights

Other fragments show completely different spectra, e.g. the object E06293A shown in Fig. 5. This magnitude 16 object is listed in the AIUB catalogue, it is in an elliptical GEO-like orbit and has an area-to-mass ratio of about 15 m^2/kg. The spectrum has a negative slope in the region from 400 nm to 800 nm, a pronounced absorption at around 820 nm, and a steep increase of the reflectance values at wavelengths larger than 820 nm. Most of the measured objects show an increasing of the

reflectance with increasing wavelength in the region between 600 nm and 900 nm. The reflectance increasing is called “reddening” and it has also been observed by other groups conducting spectroscopy observations of space objects. A possible explanation takes into account space weathering: it could be responsible for changes in the microstructure of the surface, which would cause changes in the reflectance [5]. All the observed satellites, as well as some of the debris fragments show a considerable reddening. Other objects, e.g. the observed planets, do not exhibit that effect.

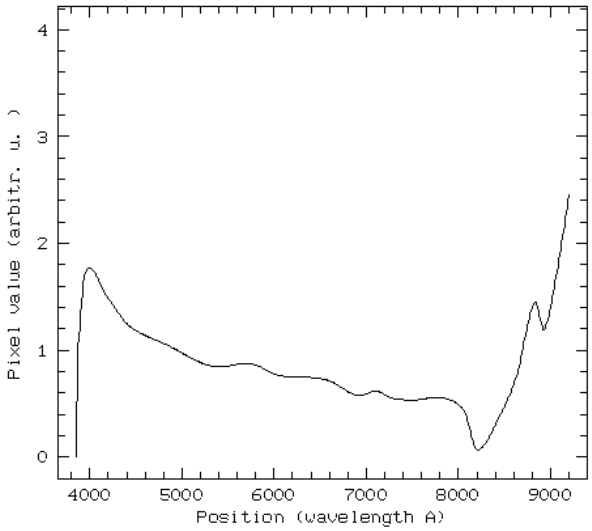

Figure 5. Spectrum of object E06293A

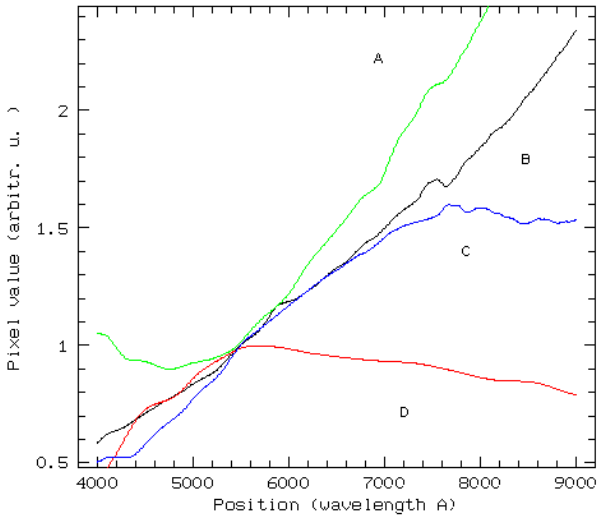

Figure 6. Spectra of the objects S92005 (A), E08211A (B), of the planets Nausikaa (C) and Pomona (D)

In Fig. 6 the spectra of the objects S92005 and E08211A (AIUB catalogue) together with measurements of the two minor planets Nausikaa and Pomona are displayed. The planet spectra reach a kind of plateau at higher wavelengths and show even a slight reflectance decrease. The existence of spectra without the reddening slope suggests that the measured effect reflects the characteristics of the material and it does not arise from a systematic error.

Some of the measured spectra show a clear dependence on the phase angle. Fig. 7 displays the spectra of a Meteosat satellite taken on different nights with varying phase angle.

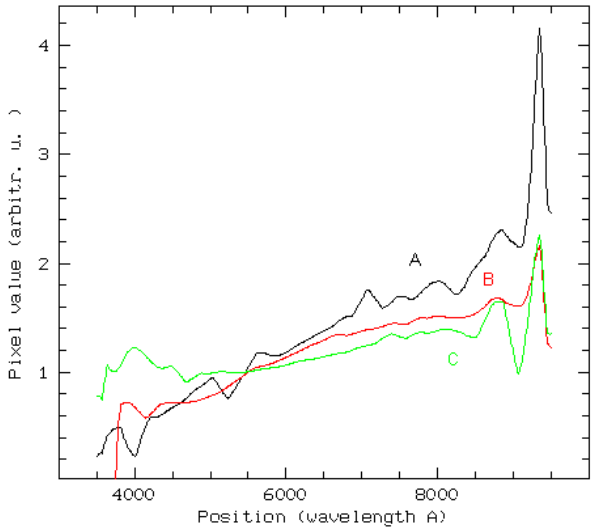

Figure 7. Spectra of a satellite Meteosat at different phase angles: 38˚ (A), 60˚ (B), 88˚ (C)

It seems that the slope of the spectrum decreases with increasing phase angles. This result is somewhat contrary to the expectations. Meteosat is a geostationary spin-stabilized satellite with its rotation axis almost parallel to the Earth’s axis and it approximately shows the observer always the same rotation-averaged face. The phase angle dependence suggests that the spectrum is determined by the scattering properties of the surface and not by the material.

Generally, the spectra may be grouped in three categories. In Fig. 8 a summary of the different types of spectra is given. The curves of the satellites Artemis and Astra are representative for the first category of spectra. The curves are convex and show a steep slope at the beginning of the infrared region, the characteristic reddening. Two instances of the second group are the spectra of the fragments E06321D and E08159C. These curves exhibit a plateau region at higher wavelengths and they are concave. The third category includes the spectra of objects like the debris fragment E04015A. Its spectrum is convex and the reflectance values decrease with increasing wavelength. In the region between 600 nm and 800 nm the spectrum becomes relatively flat.

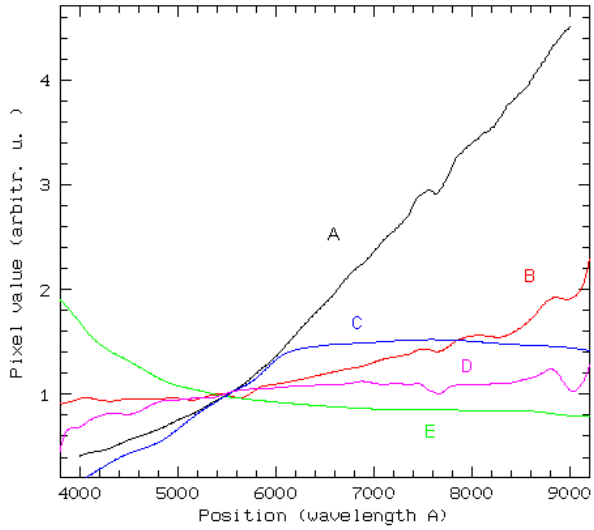

Figure 8. Spectra of satellites Artemis (A), Astra (B), and debris fragments E06321D (C), E08159C (D), E04015A (E)

6. CONCLUSIONS

Spectroscopic investigations of different satellites, debris with high area-to-mass ratio, and minor planets were performed. Faint debris fragments up to magnitude 16 could be successfully investigated. A preliminary analysis shows that it is possible to a certain extent distinguish objects on the basis of different spectra characteristics, like e.g. shape, slope, convexity, or the presence of peaks. The spectra of the same objects observed on different nights show a big analogy and similar features. Since the spectra differ sometimes only in their slope, it is very important to accurately determine the extinction function for every night. The extinction strongly depends on the observation conditions and its influence alone can be responsible for a change in the spectrum gradient.

Most of the spectra show a higher and higher reflectance with increasing wavelength. The presence of this reddening in the measurements confirms the results obtained by other research groups in similar spectroscopic investigations. The dependence of the spectra of the Meteosat satellite from the phase angle suggests that the shape of the reflectance curve is also characterized by the microstructure of the object surface. This hypothesis has been used by other authors to explain the reddening effect.

For the determination of the material from the spectroscopic measurements it is necessary to have reference spectra of the materials commonly used on spacecraft surfaces. One of the future goals is the characterization of the material of the debris fragments by means of reference spectra. The simplest case would be the identification of debris composed of a single material, e.g. aluminium. The next steps also include the improvement of the accuracy of the extinction determination and better methods for the elimination of background noise and fringes.

7. ACKNOWLEDGMENTS

The spectroscopy observations at the ESASDT telescope were acquired under the ESA contract AO/1-5538/08/F/VS. The orbits of several catalogue objects were provided by the Keldysh Institute of Applied Mathematics (KIAM) in the framework of the ISON collaboration.

8. REFERENCES

1. Schildknecht, T., Musci, R., Früh, C. & Ploner, M. (2008). Color Photometry and Light Curve Observations of Space Debris in Geo, In *Proceedings of the IAC 08, International Astronautical Congress 2008, A6.1.04*, Glasgow, UK
2. Musci, R., Schildknecht, T. & Ploner, M. (2008). Analyzing long Observation Arcs for Objects with high Area-to-Mass Ratios in geostationary Orbits, In *Proceedings of the IAC 08, International Astronautical Congress 2008, A6.1.10*, Glasgow, UK
3. Jorgensen, K. (2000). *Using Reflectance Spectroscopy to Determine Material Type of Orbital Debris*, Ph.D. Thesis, University of Colorado, Boulder, USA
4. Jorgensen, K., Okada, J., Guyote, M., Africano, J., Hall, D., Hamada, K., Barker, E., Stansbery, G. & Kervin, P. (2004). Reflectance Spectra of Human-Made Objects, In *2004 AMOS Technical Conference*, Maui, Hawaii, USA
5. Abercromby, K.J., Okada J., Guyote, M., Hamada, K. & Barker, E. (2007). Comparisons of Ground Truth and Remote spectral Measurements of FORMOSAT and ANDE Spacecraft, In *2007 AMOS Technical Conference*, Maui, Hawaii, USA
6. Banse, K., Grosbol, P., Ponz, D., Ounnas, C., Warmels, R., The MIDAS Image Processing System, In *Instrumentation for Ground Based Astronomy: Present and Future* (Ed. L.B. Robinson), Springer Verlag, New York, p. 431